The motion-induced contour revisited: Observations on 3-D structure and illusory contour formation in moving stimuli

Gennady Erlikhman Department of Psychology, University of Nevada, Reno, NV, USA

Mengzhu Fu Department of Psychology, University of Nebraska, Lincoln, NE, USA

Michael D. Dodd Department of Psychology, University of Nebraska, Lincoln, NE, USA

Gideon P. Caplovitz Department of Psychology, University of Nevada, Reno, NV, USA

The motion-induced contour (MIC) was first described by Victor Klymenko and Naomi Weisstein in a series of papers in the 1980s. The effect is created by rotating the outline of a tilted cube in depth. When one of the vertical edges is removed, an illusory contour can be seen in its place. In four experiments, we explored which stimulus features influence perceived illusory contour strength. Participants provided subjective ratings of illusory contour strength as a function of orientation of the stimulus, separation between inducing edges, and the length of inducing edges. We found that the angle of tilt of the object in depth had the largest impact on perceived illusory contour strength with tilt angles of 20° and 30° producing the strongest percepts. Tilt angle is an unexplored feature of structure-from-motion displays. In addition, we found that once the depth structure of the object was extracted, other features of the display, such as the distance spanned by the illusory contour, could also influence its strength, similar to the notion of support ratio for 2-D illusory contours. Illusory contour strength was better predicted by the length of the contour in 3-D rather than in 2-D, suggesting that MICs are constructed by a 3-D process that takes as input initially recovered contour orientation and position information in depth and only then forms interpolations between them.

Introduction

In a series of papers in the 1980s, Victor Klymenko and Naomi Weisstein explored the properties of a novel visual illusion called the motion-induced contour (MIC; Klymenko & Weisstein, 1980, 1981, 1983, 1984; Klymenko Weisstein, & Ralston, 1987). The basic effect can be seen by taking the outline of a rectangular solid, removing one of the vertical edges, and rotating the object about the axis of tilt (Figure 1 and Movie 1). The percept is of an illusory contour in the place of the missing edge. Here, we further explore stimulus factors that influence the formation and perceived strength of the MIC. The results of the four experiments described below reveal that both 2-D stimulus characteristics as well as contour relationships in inferred 3-D mediate the strength of the MIC.

In their original work, Klymenko and Weisstein (1980, 1981) sought to identify the necessary and sufficient conditions for perceiving the MIC. In most experiments, participants were simultaneously presented with five stimuli arranged in a circle. Participants would then be cued to provide a subjective rating for the strength of the illusory contour in one of the stimuli and would then provide relative ratings for each of the four other stimuli. Klymenko and Weisstein found that the MIC was perceived most strongly when the stimulus was rotated in depth and was weakly or not at all perceived when it translated, rotated in a fronto-parallel plane, or loomed toward the observer. From these observations, they concluded that the MIC did not depend on motion or rotation in general, nor did it depend on motion through depth, but on rotation through depth of the stimulus. Further experiments showed that the MIC was also not seen if the stimulus was constructed as a flat object on a plane that itself rotated through depth. That is, the perception of the illusory contour depended on motion of the stimulus,

Citation: Erlikhman, G., Fu, M., Dodd, M. D., & Caplovitz, G. P. (2019). The motion-induced contour revisited: Observations on 3-D structure and illusory contour formation in moving stimuli. *Journal of Vision, 19*(1):7, 1–17, https://doi.org/10.1167/19.1.7.

https://doi.org/10.1167/19.1.7 Received June 18, 2018; published January 16, 2019 ISSN 1534-7362

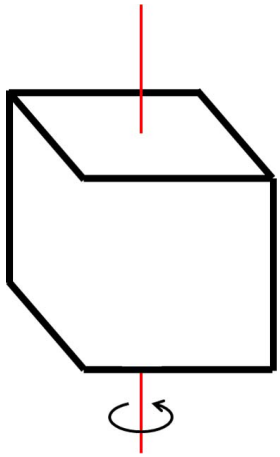

Figure 1. The MIC: The outline of a rectangular solid is tilted slightly toward the observer. The solid rotates about the axis of tilt, which passes through its center, shown here as a thin red line. Although the missing vertical edge is very faintly completed or not at all in this image, an illusory contour is clearly seen in its place when the object rotates as in Movie 1.

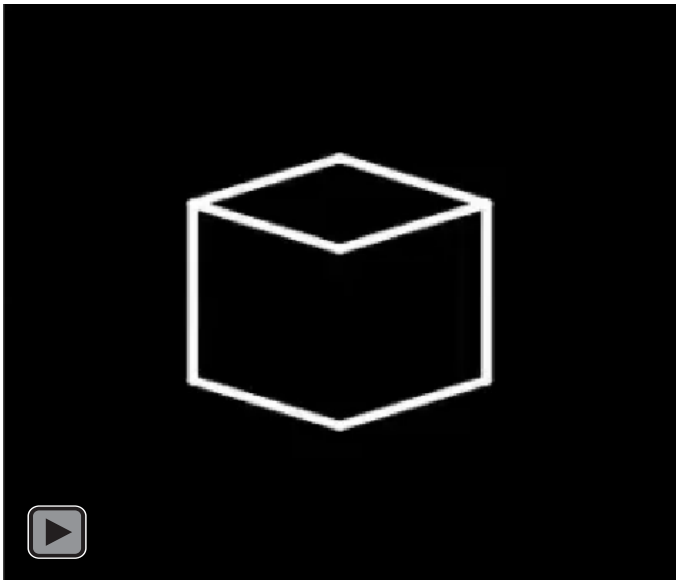

Movie 1. The Motion-Induced Contour. A rotating Necker cube with one of its vertical edges removed. An illusory contour is seen in its place.

which was consistent with that of a 3-D object rotating through depth and not just rotation through depth of any object (i.e., of a 2-D surface). Subsequent work showed that the MIC could be seen even in a simplified version of the display consisting of only two chevrons that correspond to the closest two top and two bottom edges of the cube (Figure 2 and Movie 2). In these displays, additional illusory contours can be seen along the sides of the chevron. Some image transformations, such as planar motion, affect the illusory strength of these monohedral (i.e., belonging to one surface) edges but not the dihedral (belonging to two surfaces) MIC formed between the two surfaces, suggesting that they may arise from different processes (Klymenko & Weisstein, 1984; for a detailed review of the papers on this topic, see Erlikhman & Caplovitz, 2018). Monohedral edges may arise from processes that produce

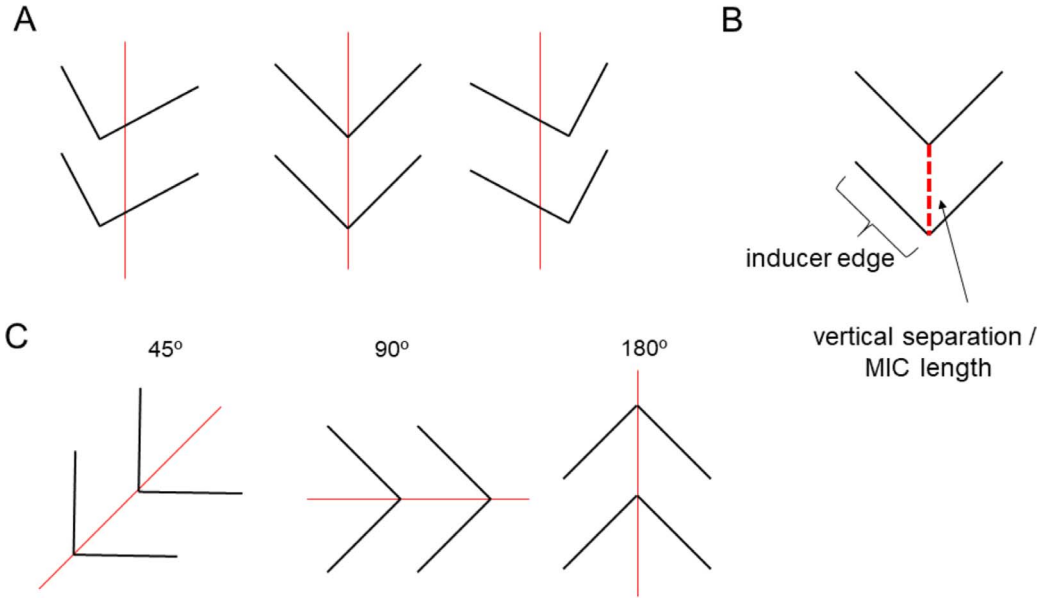

Figure 2. (A) Three frames from an animation sequence depicting two chevrons that form two pairs of edges of a cube. The chevrons rotate about the axis of tilt indicated in thin red lines. The MIC appears between the vertices of the two chevrons when they rotate (Movie 2). (B) Inducer edge length refers to the length of the visible, black contours. Vertical separation is the distance between chevron vertices indicted by the dashed red line. (C) Chevrons at different orientations.

illusory contours from motion (e.g., Anderson & Barth, 1999; Bruno & Gerbino, 1991) although edge terminators in these displays do not serve as occlusion cues and the vertices of the chevrons where the MIC is formed are not terminators.

The stimuli that give rise to the MIC share several features in common with the kinetic depth effect, in which a perception of 3-D structure arises from 2-D motion patterns (Wallach & O'Connell, 1953). Like the kinetic depth effect, MICs are only seen when the motion patterns correspond to an object rotating in depth and not when the object is translated laterally, rotated in a 2-D plane, moved in depth without rotation (i.e., looming), or set to flicker (Klymenko & Weisstein, 1981, 1983). In a majority of Klymenko and Weisstein's displays, the objects were rigid and rotated smoothly at a constant velocity. Rigidity and smoothness have been proposed as necessary constraints for the visual system to be able to recover 3-D structure from motion (Hildreth, 1984; Hoffman & Bennet, 1985, 1986; Rokers, Yuille, & Liu, 2006; Ullman, 1979, 1984a, 1984b; Zanforlin, 1988; but see Jain & Zaidi, 2011). However, although the percept of a 3-D cube in the MIC stimulus can be explained by the same processes that underlie the kinetic depth effect, they on their own do not account for the formation of an illusory contour. In considering the dependence of one effect on the other, it is clear that an illusory contour is not a necessary feature of displays in which 3-D structure is recovered from motion as many structure-from-motion displays do not also produce illusory contours. MICs (and the surfaces they are attached to) are also not subject to some of the proposed constraints on structure from motion as both they and the surfaces they abut can be nonrigid (Movie 3).

Although the 3-D structure does not depend on the perception of an illusory contour, the MIC percept may require first recovering the 3-D structure of the object. Models of 3-D contour interpolation in static displays take as initial input the positions and orientations of edges in 3-D space, and only after their arrangement in depth is established are intermediate contours interpolated (Kellman, Garrigan, & Shipley, 2005; Kellman, Garrigan, Shipley, Yin, & Machado, 2005). For stereoscopically defined edges, a 3-D illusory contour can be formed if the edges can be connected by a smooth, monotonic curve in 3-D even if their 2-D (i.e., retinal) projections are misaligned. Similarly, if the retinal projections of two edges are aligned, a 3-D illusory contour will not be formed between them if they are not similarly relatable in 3-D space (Kellman & Shipley, 1991). This suggests that the visual system first recovers the 3-D structure of a scene and only then forms illusory contours in unifying spatially segregated surfaces into single objects. For the MIC, the rotation in depth of the real, luminance-defined edges of the object is necessary to first recover the overall 3-D structure, and only then does an additional process form the illusory contour.

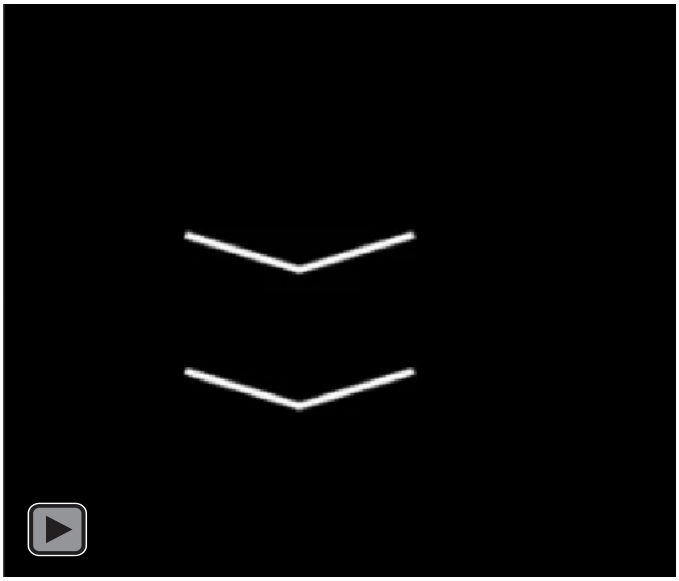

Movie 2. Motion-induced contour formed by only two "chevrons" formed from four edges of the cube.

Once illusory contours are formed, they may interact with other processes. For example, both stationary and moving, illusory and amodally completed figures can affect surface segmentation and integration by "capturing" other surfaces (Ramachandran, 1986; Yin, Kellman, & Shipley, 2000). Stationary and moving illusory contours can be integrated with real, motion-defined, or other illusory contours (Poom, 2001a, 2001b). And, like real contours, illusory contours can be integrated over time to form dynamically defined figures (McCarthy, Erlikhman, & Caplovitz, 2017; McCarthy, Strother, & Caplovitz, 2015). Although it may, therefore, be the case that the illusory contour in MIC has some reciprocal effect on the perception of the form of the object or its motion, it should be noted that the MIC is not seen when the object is stationary as in Figure 1. It is, therefore, likely that the structure of the real visible edges is recovered first, after which the illusory contour is formed.

In this paper, we sought to explore this second aspect of the MIC. Whereas Klymenko and Weisstein focused on the features that influenced the recovery of 3-D structure, here we examine what features may influence perceived illusory contour strength after the 3-D configuration of the luminance-defined edges has already been recovered. In particular, we were interested in whether some of the properties that are known to influence illusory contour strength in 2-D displays, such as support ratio—the ratio of visible to invisible edge length—apply in three dimensions (Shipley & Kellman, 1992). It is unclear whether support ratio

would be a relevant feature for MICs because, unlike 2-D illusory contours, MICs do not lie on the same plane as the visible, inducing edges. In 2-D displays, L- and T-junctions (tangent discontinuities) may serve as occlusion cues for initializing illusory contour formation or as occlusion cues (Gillam, 1987; Kellman & Shipley, 1991; Rubin, 2001; Shipley & Kellman, 1990). Junctions and occlusion cues can also be used to form 3-D illusory contours and illusory surfaces and volumes (Carman & Welch, 1992; Tse, 1998, 1999, 2017a, 2017b). However, the MIC is not attached to an occluding surface and in that sense differs from other kinds of illusory contour displays.

In the first experiment, we explored the effects of inducer edge length, inducer separation, and stimulus orientation on perceived illusory contour strength. Inducer edge length and separation were used to compute support ratio. To anticipate our results, we found that illusory contour strength ratings of MICs increased as a function of support ratio, just as for 2-D contours. We also found an unexpected effect of orientation in that when the MIC stimulus was horizontal, ratings were overall lower than for other orientations. Support ratio was computed based on inducer and illusory contour length as defined in 3-D. Changing the illusory contour length by manipulating the distance between inducing edges increases both the 2-D separation (on the screen and retina) and the 3-D size of the object. In Experiment 2, 2-D and 3-D separations were manipulated independently, allowing us to distinguish between retinal and object-based support ratio. In order to achieve this, the object had to be tilted by different degrees. Surprisingly, illusory contour strength ratings were found to decrease as a function of increasing 3-D length but increased as a function of 2-D length. That is, the farther apart the two inducing edges were in depth, the harder it was too see the contour, but the farther apart they were on the screen, the easier it was to see the contour. The effects could be explained by looking at the tilt angle of the object, which was manipulated in order to achieve different 2-D and 3-D separations. The strength of the illusion was most strongly predicted by tilt angle, which, to our knowledge, is typically not considered in structure-from-motion displays. In Experiment 3, we show that these effects are not due to the object rotating through a greater distance in depth as tilt increases. In the last experiment, we confirmed that, in addition to tilt angle, other stimulus features, such as 3-D separation do independently influence perceived illusory contour strength. Taken together, the results of these experiments suggest an important role for the recovery of 3-D shape through an analysis of motion not as the end state of object representation, but as an integrated part of ongoing perceptual processing that can subsequently lead to the formation of illusory contours (Erlikhman, Caplovitz, Gurariy, Medina, & Snow, 2018).

Experiment 1

Subjective ratings of MIC strength were measured as a function of the orientation of the stimulus, the length of the inducers (i.e., visible edges), and the vertical separation between inducers (i.e., length of the MIC). In all experiments, a simplified version of the original display was used in which only two pairs of edges are shown, each pair of which defines a corner of a cube (Figure 2 and Movie 2). This display, in which pairs of edges appear as chevrons, produces comparable MICs and is devoid of contextual cues, such as additional edges and surfaces of the object, which may interact with MIC perception (Erlikhman & Caplovitz, 2018; Klymenko & Weisstein, 1983). Inducer edge length and vertical separation were used to compute support ratio (described below). Stimulus orientation was manipulated because all previous experiments on MIC have used "upright" figures (Klymenko & Weisstein, 1981, 1983, 1984), and there may have been unexpected interactions with how easily the 3-D structure of the chevrons could be extracted.

Materials and methods

Apparatus

All stimuli were created on MATLAB (MathWorks, Natick, MA) using the Psychophysics Toolbox (Brainard, 1997; Pelli, 1997). Stimuli were presented on a computer running Windows 10 64-bit, powered by an Intel Xeon E5603 CPU with 1.6 Hz quad-core and an NVIDIA Quadro 600 1-GB graphics card. A 23-in. Dell U2312HM LCD monitor was used with a resolution set to 1,920 × 1,080 with a refresh rate of 60 Hz.

Participants

Participants were 32 undergraduate students at the University of Nebraska, Lincoln, who participated for course credit. All had normal or corrected-to-normal vision and were naïve to the purposes of the study. All experiments were carried out in accordance with the Code of Ethics of the World Medical Association (Declaration of Helsinki) and were approved by the University of Nebraska, Lincoln, institutional review board (IRB). All participants provided informed consent. In determining the number of desired participants, our goal was to collect data from at least 10, which was the number originally used by Klymenko

and Weisstein (1981). Participants were recruited via the university's online subject recruitment system for which many sign-up slots were opened simultaneously. A larger number of participants than expected signed up for this and the other experiments, thus leading to uneven sample sizes across Experiments 1 through 4. Rather than arbitrarily select and analyze subsets of the collected data to maintain equal sample sizes, we report all of the collected data.

Stimuli

The cube was initially defined in 3-D coordinates so that one of its vertical edges was facing the observer. It was then tilted by 20° about the *x*-axis (i.e., pitched forward toward the observer). All edges of the cube were then removed except two of the top edges and two of the bottom edges, resulting in two chevrons (Figure 2A). A parallel projection was used to display the cube on the screen. During the course of a trial, the chevrons rotated by 1° per frame about the axis of tilt, up to 20° clockwise or counterclockwise, at which point the rotation direction reversed. This corresponded to a rotational velocity of 60° per second. Initial rotation direction was randomized. Chevrons were white on a black background and appeared centered on the screen.

Three features of the stimulus were parametrically varied: the vertical separation between the chevrons, the length of each inducing edge comprising the chevrons, and the orientation of the entire stimulus. Vertical separation was computed as the projected distance between the top and bottom of chevrons if they had not been titled and rotated. This corresponded to their inferred separation in 3-D. The three separations were 1.52°, 2.54°, and 3.55° of visual angle. It was also possible to compute the vertical separation as the projected distances onto the monitor between the chevron vertices after they had been tilted. Those distances were 1.43°, 2.38°, and 3.34°. However, this latter measurement is difficult to use consistently because, as the chevrons rotate, the projected lengths of the edges change. This effect can be seen in the images from the animation sequence in Figure 2A. Therefore, in all subsequent figures and calculations, we use the former, inferred 3-D distances and not the latter, 2-D projections. We consider the difference between these two measurements in Experiment 2. Inducer edge length was likewise computed as the inferred 3-D length of the edges if the chevron was not rotated or tilted. The four lengths used were 0.56°, 1.19°, 1.79°, and 2.54°. For the orientation manipulation, the entire object was rotated about its *z*-axis by 0°, 45°, 90°, or 180°. The 180° rotation amounted to flipping the display upside down, and, thus, as illustrated in Figure 2C, both the 0° and 180° rotations induce a vertical MIC, the 45° rotation induces an oblique MIC, and the 90° rotation induces a horizontal MIC. In all cases, the stimulus was always first rotated by 20° about the *x*-axis (tilted forward) and only then was the second rotation applied. The direction of rotation—clockwise or counterclockwise (up/down in the 90° condition)—was randomized on each trial. All conditions were manipulated independently, resulting in 48 unique combinations, each of which was repeated four times during the course of the experiment. The presentation order was pseudorandomized.

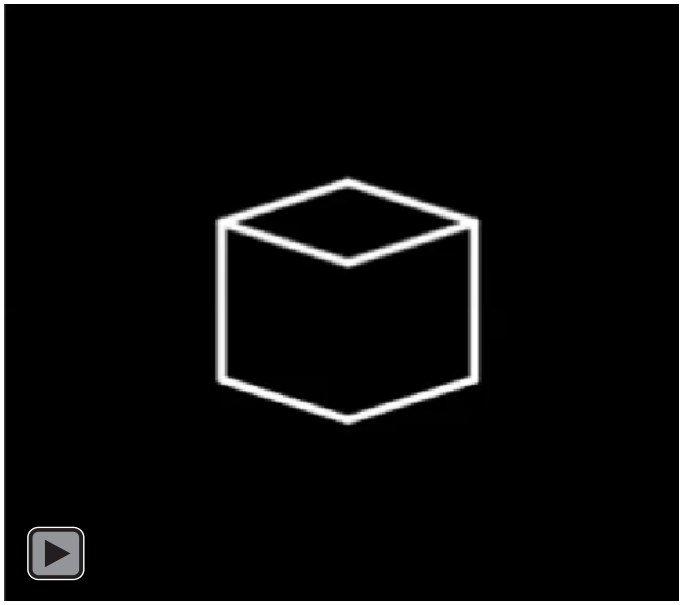

Movie 3. Non-rigid motion-induced contour. As in Movie 1, but the top and bottom parts of the cube rotate in opposite directions. The illusory edge appears to twist.

Procedure

At the beginning of the experiment, participants saw an instruction screen on which they were told that the goal of the study was to rate the strength of a visual illusion. They were then shown an example of a Kanizsa square, and illusory contours in the figure were pointed out although the term "illusory contour" was never used (Kanizsa, 1955, 1979). Then, a subjective Necker cube display was shown to illustrate that such contours could appear in 3-D (Bradley, Dumais, & Petry, 1976; Bradley & Petry, 1977). This display consisted of a white Necker cube on a white background with black circles behind each of the vertices. They were then shown two animated displays. As illustrated in Figure 1, one was the MIC display with all sides of the cube visible except for the front edge (0° rotation, vertical separation = 2.54°, inducer edge length = 1.19°, tilt angle = 20°). On a scale from zero to seven, participants were instructed that the strength of the illusion would correspond to a seven.

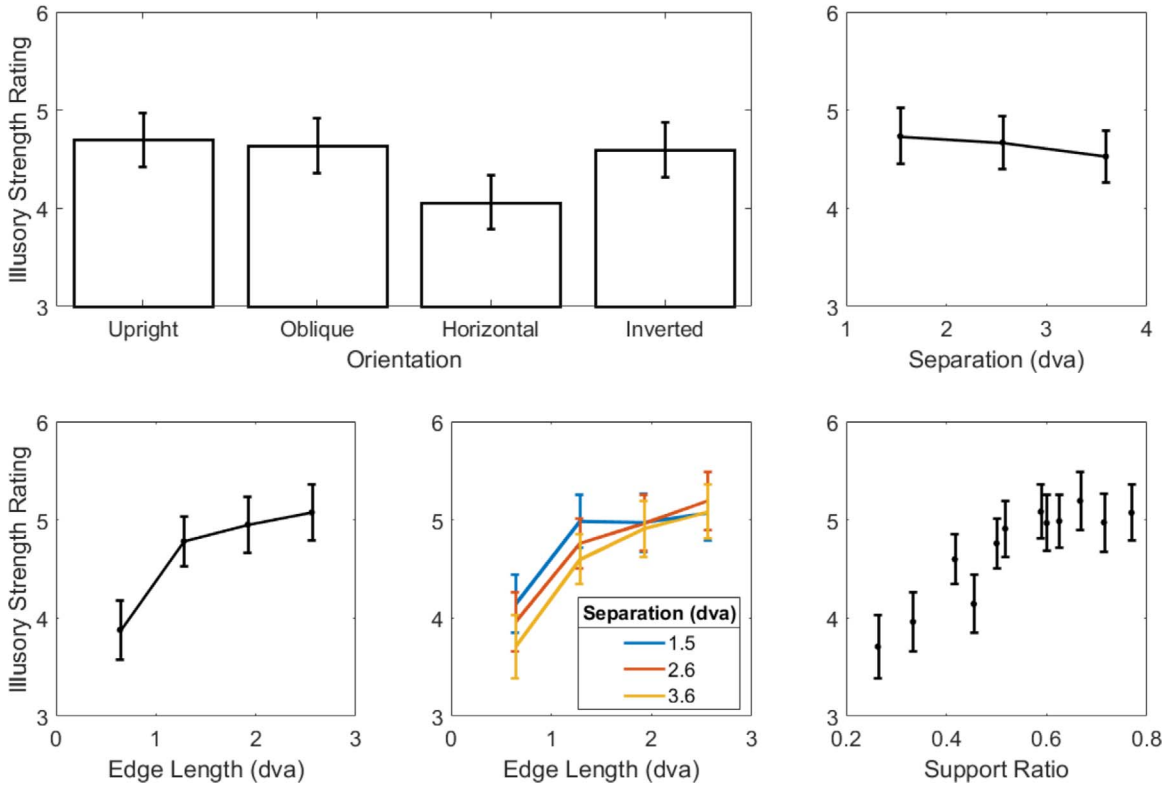

Figure 3. Top row: Effect of orientation and vertical separation between chevrons on MIC strength ratings. DVA = degrees of visual angle. Second row (left to right): Main effect of visible (chevron) edge length, interaction between edge length and vertical separation, and support ratio. Error bars are standard errors.

The second display was the same except with large circles added to each of the cube's vertices. This prevented the formation of illusory contours, and participants were told that it corresponded to a rating of zero. Both animations were on the screen at the same time so that participants could compare between the two, and both remained on the screen until participants made a key press to begin the experiment. After a 300-ms pause in which a blank black screen was shown, a stimulus then appeared in the middle of the screen and continued to rotate back and forth until a number rating was provided with a keyboard key press between zero and seven. Following a key press, another blank black screen was shown for 300 ms, after which the next trial began. There were no breaks, and the entire experiment lasted for approximately 20 min.

Results

For each participant, the average rating was computed across the four repetitions of each of the 48 conditions. Because ratings were bounded and there were several participants who often gave ratings of seven, we applied a logit transform to the rating data.[1] For data points that were exactly zero or seven, data were adjusted up or down by 0.1, respectively, to prevent infinite values after transformation. Group averages and standard deviations of the transformed data were used to assess the main effects and interactions of the three stimulus manipulations on the strength of the MIC. However, for ease of visual examination, figures show untransformed ratings. Main effects are shown in the first three panels of Figure 3. Ratings were not affected by stimulus orientation—except for a dip in the 90° rotation (i.e., horizontal) condition—but decreased as a function of separation and increased as a function of edge length. Statistical significance of these main effects and the interactions between the three factors were determined by a 4 (orientation) × 3 (separation) × 4 (edge length) repeated-measures ANOVA. Greenhouse–Geisser correction was applied to all tests. There were significant main effects of each of the variables on MIC strength ratings: orientation, $F(1.84, 57.29) = 12.60$, $p < 0.001$, $\eta_p^2 = 0.289$; separation, $F(1.28, 39.67) = 5.27$, $p = 0.020$, $\eta_p^2 = 0.145$; and inducer length, $F(1.19, 36.86) = 26.78$, $p < 0.001$, $\eta_p^2 = 0.463$. A two-way interaction was observed between edge length and separation, $F(4.37, 135.61) = 4.41$, $p = 0.002$, $\eta_p^2 = 0.125$, but not between edge length and orientation, $F(6.16, 191.02) = 1.60$, $p = 0.142$, $\eta_p^2 = 0.050$, or separation and orientation,

$F(4.55, 141.08) = 1.05$, $p = 0.388$, $\eta_p^2 = 0.033$. There was no significant three-way interaction, $F(8.86, 274.62) = 0.640$, $p = 0.760$, $\eta_p^2 = 0.020$.

The interaction between edge length and separation can been seen in the fourth panel of Figure 3: The MIC was rated as being stronger when the separation between inducers was smaller; however, this was only the case for the shorter two edge lengths. At the larger edge lengths, all separations were rated as equally strong, likely suggesting a perceptual ceiling for the strength of the MICs had been reached. We repeated the analysis, excluding the 90° condition, to see if it alone was responsible for the main effect of orientation. When excluded, there was no main effect of orientation, $F(1.54, 47.81) = 0.94$, $p = 0.376$, $\eta_p^2 = 0.029$, and no interaction between orientation and separation, $F(3.28, 101.80) = 1.17$, $p = 0.329$, $\eta_p^2 = 0.036$, or between orientation and edge length, $F(4.33, 134.24) = 1.13$, $p = 0.345$, $\eta_p^2 = 0.035$, whereas the main effects of edge length and separation remained as well as the interaction between them: edge length, $F(1.23, 38.09) = 28.01$, $p < 0.001$, $\eta_p^2 = 0.475$; separation, $F(1.41, 43.72) = 5.37$, $p = 0.016$, $\eta_p^2 = 0.148$; separation × edge length, $F(4.86, 150.74) = 4.64$, $p = 0.001$, $\eta_p^2 = 0.130$. The three-way interaction was not significant, $F(7.18, 222.46) = 0.60$, $p = 0.758$, $\eta_p^2 = 0.019$. This suggests that the 90° condition was indeed driving the main effect of orientation and likely represents a special case of the MIC.

For each display, support ratio was defined as the ratio of the length of the real (i.e., luminance-defined) contour to the total contour length (i.e., real + illusory) as in Shipley and Kellman (1992). Real contour length was computed as double the inducer edge length, assuming that one edge on either side of the MIC served as an inducer. Illusory contour length was the vertical separation between chevrons. Both real and illusory contour length were based on their inferred 3-D size as described above. Analogous to static illusory contours, MIC strength ratings increased as a function of support ratio. This was the case here up to a ratio of approximately 0.6, after which the ratings reach an asymptote (bottom right panel of Figure 3).

Discussion

MIC strength increased as a function of edge length and decreased as a function of vertical separation between chevrons. When these variables were combined into a single variable of support ratio, a clear, linear trend was seen, up to ratios of ~0.6. As with the 2-D support ratio, the larger the proportion of the illusory contour that must be interpolated, the weaker its perceived strength (Shipley & Kellman, 1992). The leveling off at higher support ratios may reflect an upper limit in the clarity of the MIC displays used in this experiment relative to the comparison stimulus shown in the instructions at the beginning of the experiment, which guided the maximum of the rating scale. It is also interesting to note that the effect of support ratio seems to be mainly driven by inducer edge length and not by vertical separation (compare the bottom left panel of Figure 3 to the top right).

MIC strength was unaffected by stimulus orientation except for when the display was horizontal (90°). It is not obvious why the horizontal orientation would systematically produce lower ratings. For static, 2-D contours, there is no difference in perceptibility of horizontal versus vertical illusory contours as measured by orientation discrimination thresholds (Vogels & Orban, 1987). Klymenko and Weisstein did not explicitly test the effect of overall stimulus orientation, and at present, we do not have a compelling explanation for why this difference in MIC strength based on orientation might occur. As such, we have excluded stimulus orientation in subsequent experiments, but note that vertical/horizontal anisotropies have been observed in other domains in 3-D perception (Cagenello & Rogers, 1993; Gillam & Ryan, 1992; Mitchison & McKee, 1990; Rogers & Graham, 1983; Wallach & Bachon, 1976), and this factor may well be worth further empirical study.

Experiment 2

The results of Experiment 1 are consistent with findings of support ratio as being the determining factor of MIC strength ratings. In computing support ratio, both real and illusory contour lengths were determined from inducer edge length and vertical separation as inferred in 3-D. If the visual system first recovers the arrangement of chevrons in depth and then uses this information to interpolate the MIC, then using the inferred distances in depth may have been appropriate. However, the visual system might also complete the MIC in retinal coordinates before or at the same time as determining the depth relations in the scene. In this latter case, perhaps the 2-D projection of the distance between the chevrons may have been the determining factor influencing MIC strength. In Experiment 1, 3-D and 2-D separations were confounded in that both increased as the chevrons were moved apart. In Experiment 2, we designed displays in which these two properties could be manipulated independently. By changing the degree of tilt of the object, it was possible to keep fixed the 2-D distance between the chevron vertices while changing the 3-D size of the object. That is, the separation between the chevrons

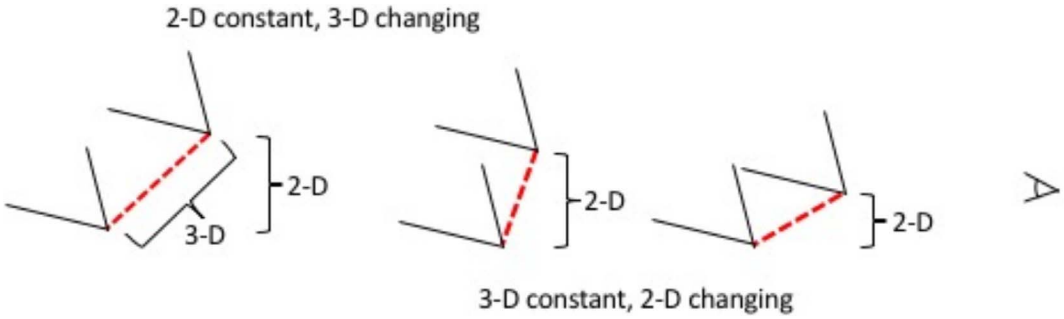

Figure 4. Effect of holding either 2-D or 3-D separation between vertices constant while manipulating the other. The red dashed line indicates the MIC. Its length is the 3-D separation. The 2-D separation is the vertical distance between the chevron vertices after parallel projection onto the screen and indicated by the bracket on the right of each stimulus. For the leftmost and central images, the 2-D separation remains constant while the 3-D separation changes. For the central and right images, the 3-D distance is constant while the 2-D separation decreases as the entire stimulus becomes more tilted. The observer is indicated by the eye on the right.

was increased in depth but not vertically on the screen. Likewise, it was possible to keep 3-D separation fixed but to change 2-D size by tilting the object toward the observer. If the visual system first extracts depth information about the scene before forming the MIC, then the strength of the illusion should decrease as 3-D separation increases but should not be affected by changing the 2-D separation while keeping the other fixed.

Materials and methods

Participants

Participants were 14 undergraduate students at the University of Nebraska, Lincoln, who participated for course credit. All had normal or corrected-to-normal vision and were naïve to the purpose of the study. All experiments were carried out in accordance with the Code of Ethics of the World Medical Association (Declaration of Helsinki) and were approved by the University of Nebraska, Lincoln, IRB. All participants provided informed consent.

Stimuli and procedure

The testing apparatus and procedure were the same as for Experiment 1. The only difference was in the sizes and orientations of the stimuli that were presented. Either 2-D separation between inducers was varied while 3-D separation was fixed or vice versa (Figure 4). Six different 2-D separations, 2.54°, 3.80°, 5.07°, 5.70°, 6.33°, and 6.97° of visual angle, were paired with a fixed 3-D separation of 7.60°. In this case, the 2-D separations indicate retinal distance between inducers after the object has been tilted and projected into two dimensions, and the 3-D separation represents inferred size of the object if it were not tilted as in Experiment 1. Knowing the length of the projection of the separation onto the screen and the 3-D distance, it was possible to compute the angle at which the stimulus was tilted toward the observer (i.e., rotated about the x-axis). For example, if the stimulus was not tilted at all (tilt angle = 0°), the 2-D and 3-D separations would be equal. As the stimulus is tilted toward the observer, the 3-D distance between the inducers remains constant while the 2-D distance between them decreases. From this, one can see why 2-D separation can only be equal to or smaller than the 3-D separation. For each of the 2-D separations, the corresponding tilt angles were 70.53°, 60°, 48.19°, 41.41°, 33.56°, and 23.56°, respectively, where 0° corresponded to an upright stimulus that was not tilted. Smaller 2-D separations required larger tilts.

For these fixed 3-D separation conditions, three edge lengths were used: 2.54°, 3.80°, and 5.07°. Each combination of 2-D separation and edge length was tested, resulting in 18 unique stimuli. Because our definition of the support ratio is based on the inferred 3-D separation of the inducers and the 3-D separation was kept constant, the support ratio remained the same for each edge length regardless of 2-D separation, and longer inducing edges increased the support ratio.

In the other condition, 2-D separation was fixed while 3-D separation was allowed to vary. Six 3-D separations were used: 5.70°, 6.33°, 6.97°, 7.60°, 8.86°, 10.12°, which were each paired with a fixed 2-D separation of 5.07°. Again, the 3-D separation is the inferred height of the untilted stimulus, and 2-D separation is the retinal distance between chevron vertices. Tilt angles for each stimulus in this condition were 27.27°, 36.87°, 43.34°, 48.19°, 55.15°, and 60° for each of the 3-D separations, respectively. These angles were specifically selected so that the 2-D separation of the inducers remained fixed. A longer stimulus had to be tilted more to project to the same retinal size as a small stimulus. Thus the 5.70° 3-D stimulus was always presented with a tilt angle of 27.27°, and the 10.12° 3-D

stimulus was always presented with a tilt angle of 60°. Larger stimulus sizes were used compared to Experiment 1 to allow for a greater range of tested values and because the 3-D separation always had to be larger than the 2-D separation.

For this condition, inducer edge length was also varied but was defined relative to 3-D separation. This way, for very large or very small separations, the inducing edges would not be disproportionally longer or shorter, avoiding extreme support ratios. Inducer edge length in degrees of visual angle was determined in the following way: short: 0.5 × (3-D separation) − 1.27°; medium: 0.5 × (3-D separation); long: 0.5 × (3-D separation) + 1.27°. As a result, for medium inducer edge lengths, the support ratio was always 0.5. The six 3-D separations and three edge length manipulations resulted in 18 unique trial types. When combined with the 18 trials in which 2-D separation varied, there were 36 total conditions. Each trial was repeated four times. The order of trials was pseudorandomized.

Results

The data were considered separately depending on whether the 2-D or 3-D separation varied. As in the previous experiment and for all subsequent experiments, data were first logit transformed and a Greenhouse–Geisser correction was applied to all ANOVAs. Data were submitted to a 6 (2-D separations) × 3 (inducer edge length) repeated-measures ANOVA. There was no main effect of 2-D separation distance, $F(1.48, 19.22) = 2.80$, $p = 0.098$, $\eta_p^2 = 0.177$, or of inducer length, $F(1.74, 22.61) = 1.73$, $p = 0.202$, $\eta_p^2 = 0.117$, and no interaction, $F(3.80, 49.36) = 2.09$, $p = 0.099$, $\eta_p^2 = 0.139$. Because there was no effect of inducer edge length, data are shown separately for all conditions in the top row of Figure 5 and combined across edge length in the bottom row.

The same analysis was then applied to the data with which 3-D separation varied and 2-D separation was fixed. Because inducer edge length varied with 3-D separation, we redefined the edge length variable to be three levels: short, medium, and long, where the medium length corresponded to an edge length that yielded a support ratio of 0.5, the short length corresponded to a smaller support ratio, and long corresponded to the larger support ratio. In actuality, within the "short" condition, edge length varied as a function of 3-D separation. As with 2-D separation, data were submitted to a 6 (3-D separation distance) × 3 (relative inducer edge length) repeated-measures ANOVA. There was a main effect of 3-D separation, $F(2.24, 29.17) = 4.74$, $p = 0.014$, $\eta_p^2 = 0.267$, but no effect of relative inducer edge length, $F(1.37, 17.88) = 1.98$, $p = 0.175$, $\eta_p^2 = 0.132$, and no interaction, $F(3.58, 46.55) = 0.829$, $p = 0.503$, $\eta_p^2 = 0.060$. The pattern of results was qualitatively opposite from those with 2-D separation: MIC ratings *decreased* with increasing 3-D separation (Figure 5, right panel).

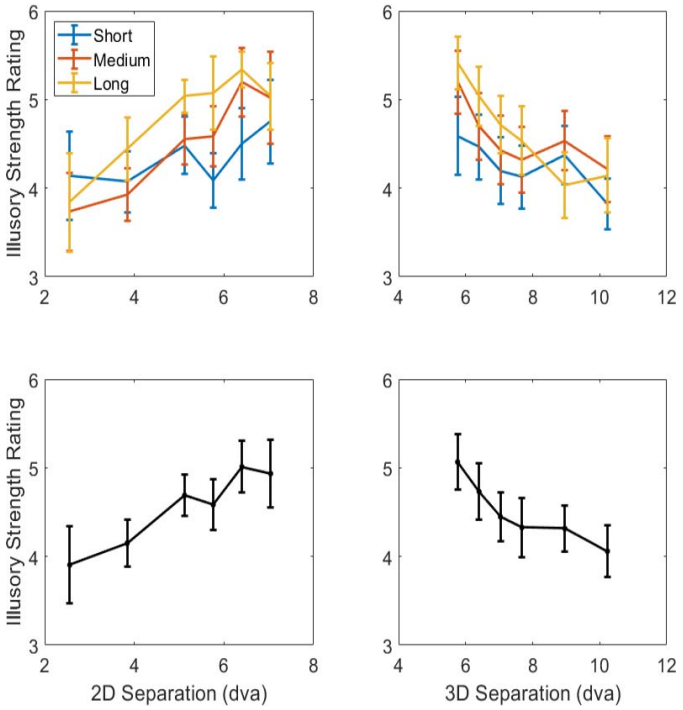

Figure 5. MIC strength ratings from Experiment 2. Top: Data for 2-D (left) and 3-D separation (right) with the other fixed. Bottom: Same data averaged across inducer edge length. Error bars are standard errors.

Discussion

In Experiment 1, MIC strength ratings increased with increasing inducer edge length and decreased as the separation between the chevrons became larger. Because the amount by which the object was tilted was constant, larger separations between chevrons corresponded to a larger distance between them both on the screen (2-D separation) and in the size of the object (3-D separation). Therefore, it was not clear whether the MIC depended on the 2-D or 3-D separation between the chevrons or possibly both. In this experiment, 2-D and 3-D separations were manipulated independently.

In agreement with Experiment 1, when 3-D separation increased, MIC strength decreased. This suggests that MIC strength is determined by real and illusory contour length *in depth* and not 2-D projected distance on the screen. That is, the visual system first recovers the 3-D structure of the scene and positions of contours in depth and only then completes illusory contours between inducing elements.

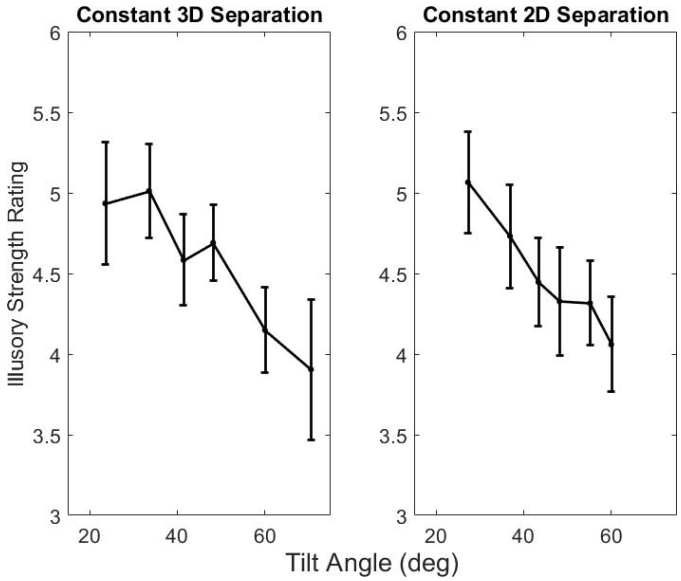

Figure 6. Data from Experiment 2 replotted as a function of tilt of the stimulus toward the observer. Tilt corresponds to rotation of the stimulus about the *x*-axis. Upright = 0°. Data are collapsed across inducer length. Error bars are standard errors.

Illusory strength ratings did not decrease with increasing 2-D separation when 3-D separation was fixed. In fact, there was a paradoxical trend in the data that ratings *increased* with increasing separation (Figure 5, lower left panel). That is, the farther apart on the screen that two inducing chevrons were placed, the stronger the MIC percept. Regardless of whether increasing 2-D separation increased ratings or had no effect, either finding is inconsistent with the basic support ratio results that increasing the separation should *decrease* illusory strength ratings (Shipley & Kellman, 1992). Why might a different pattern of results be seen here? In Experiment 1, as both 2-D and 3-D separation were increased, the overall tilt of the object remained constant at 20°. In this experiment, in order to keep one form of separation fixed while changing the other, the tilt of the object also had to be changed. For example, as 2-D separation increased, the stimulus became less tilted. Recall that 2-D and 3-D separations are equal when the object is not tilted at all (tilt is 0°). In order to keep 3-D separation fixed but change 2-D separation, the object needs to be tilted toward the observer. At extreme tilts, the 2-D separation between chevron vertices is very small. For the two shortest separations, for example, the object had to be tilted by 70.53° and 60°. In order to explore the effect of tilt on MIC strength, the data from Figure 5 were replotted in Figure 6 as a function of the tilt angle: the amount by which the chevrons had to be rotated about the *x*-axis in order to produce the desired 2-D and 3-D separations.

For both 2-D and 3-D separations, the more the stimulus is tilted (the larger the tilt angle), the lower the illusory strength rating. These data suggest that there may be two competing factors that influence MIC strength. The first, tilt angle, determines how clearly the depth relations between chevrons can be recovered. Once recovered, the strength of the MIC depends not on their projected distance (2-D separation), but, rather, on their distance in depth (3-D separation). We explore these two factors in Experiments 3 and 4.

Experiment 3

Why might tilt angle influence the perception of depth in these displays? One possibility is that increasing the tilt angle decreased the amount of motion through depth undergone by the chevron vertices. Consider an upright, untilted cube that is rotating about the vertical axis. Its corners trace a circular path through depth as it rotates. The diameter of this path is the diagonal of the cube and represents the maximum distance between the nearest and farthest point of the cube at any time during its rotation. As the cube tilts forward toward the observer, the circular path tilts forward as well, and the distance between the nearest and farthest point on the path becomes shorter, resulting in less motion through depth over the course of the rotation. The distance, D_I, that a point travels in depth in a full rotation (i.e., the distance between its nearest and farthest position relative to the observer) is given by the following equation:

$$D_I = \frac{L}{\sqrt{2}}\cos\theta,$$

where L is the length of the side of the cube and θ is the tilt angle. $\frac{L}{\sqrt{2}}$ is half of the cube's diameter and corresponds to the radius of the circular path that its corner traverses (Figure 7, left panel). As the angle of tilt, θ, increases, $\cos\theta$ decreases from one to zero, and, correspondingly, D_I also decreases.

In Experiment 2, as the chevrons became more tilted, their vertices traveled a smaller distance in depth, perhaps weakening the perception of the 3-D structure of the stimulus. In order to test this possibility, we disentangled the tilt angle from the axis of rotation. In Experiment 3, the chevron stimuli were tilted about the *x*-axis by different amounts, just as in Experiment 2, but rotated about the vertical axis, not the axis of tilt. When the axis about which the chevrons rotate is vertical, increased tilt leads to increased motion

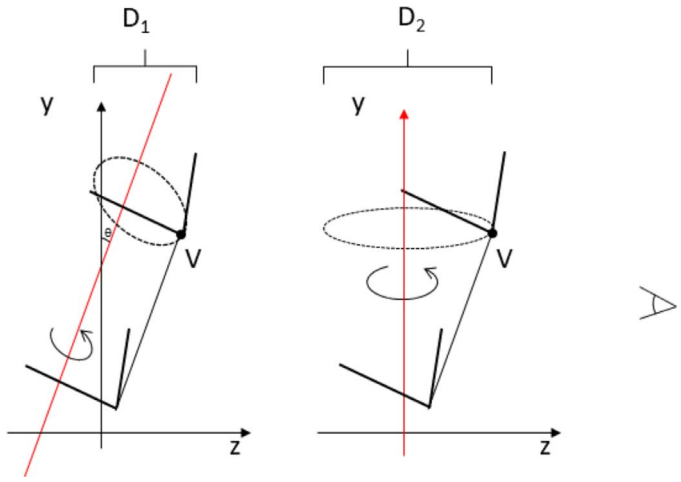

Figure 7. Motion through depth of a chevron vertex, *V*, as a function of whether the chevron is rotating about the axis of tilt (left panel) or about the vertical, *y*-axis (right panel). The dashed red line is the MIC. The observer is represented by the eye on the right. The solid red line indicates the axis about which the chevrons are rotating. The dashed oval represents the motion path of the vertex. D_1 and D_2 are the distances, in depth, between the nearest and farthest points from the observer through which the vertex, *V*, will travel. Theta is the tilt of the object, which, in this figure, is set to 20°. See text for details.

through depth. In the left panel of Figure 7, the dashed circle depicts the trajectory of a vertex, *V*, of a chevron (or the corner of a cube) as it rotates about the axis of tilt. The right panel of Figure 7 depicts the trajectory of the same vertex if the chevron/cube was rotating about the vertical, *y*-axis. This is a side-on view with the observer represented by the eye on the right and the *z*-axis being the axis through depth. D_2, the distance traveled by vertex *V* when it rotates about the *y*-axis, is larger than distance D_1 traveled by the same vertex when it rotates about the axis of tilt.

The distance traveled by vertex *V* when the chevrons are rotating about the vertical axis (Figure 7, right panel) is specified by the following equation:

$$D_2 = \frac{L}{\sqrt{2}} \sin\theta$$

where L is again the length of the MIC and θ is the angle of tilt. Comparing the equations for D_1 and D_2, one can see that as θ increases, D_1 decreases—which is what happened in Experiment 2—while D_2 increases. If the weakening of the MIC percept in Experiment 2 was due to a reduction in the amount of motion in depth as a function of tilt angle, then increasing the amount of motion in depth should increase the MIC percept. The two different motion types are shown in Movie 4.

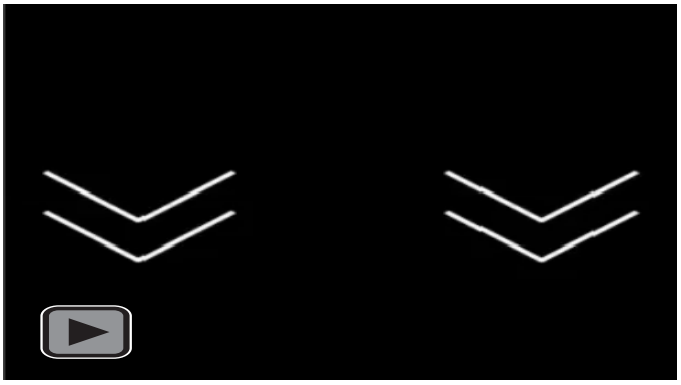

Movie 4. Rotation about the vertical axis (left) and about the axis of tilt (right).

Materials and methods

Participants

Participants were 38 undergraduate students at the University of Nebraska, Lincoln, who participated for course credit. All had normal or corrected-to-normal vision and were naïve to the purposes of the study. All experiments were carried out in accordance with the Code of Ethics of the World Medical Association (Declaration of Helsinki) and were approved by the University of Nebraska, Lincoln, IRB. All participants provided informed consent.

Stimuli and procedure

The testing apparatus and procedure were the same as for Experiment 1. Separation between edges and the tilt of the object were manipulated. The object was tilted by 20°, 40°, or 60° about the horizontal, *x*-axis, toward the observer. The vertices were separated in 3-D by 1.52°, 2.54°, or 3.55° of visual angle. The 2-D separation (retinal projection) varied as a function of tilt angle. The critical difference in this experiment was that objects rotated about the vertical, *y*-axis (alias or passive transformation) instead of about the axis of tilt (alibi or active transformation). The three separations and three tilts formed nine unique conditions, each of which was repeated four times in an experimental session. The order of trials was pseudorandomized.

Results and discussion

The results of Experiment 3 are shown in Figure 8, shown separately in the top row and combined across conditions in the bottom row. The data were submitted to a 3 (3-D separation) × 3 (tilt angle) repeated-measures ANOVA. There was a main effect of tilt angle, $F(1.17, 43.30) = 34.73$, $p < 0.001$, $\eta_p^2 = 0.484$, but not of separation, $F(1.38, 51.24) = 2.15$, $p = 0.141$, $\eta_p^2 =$

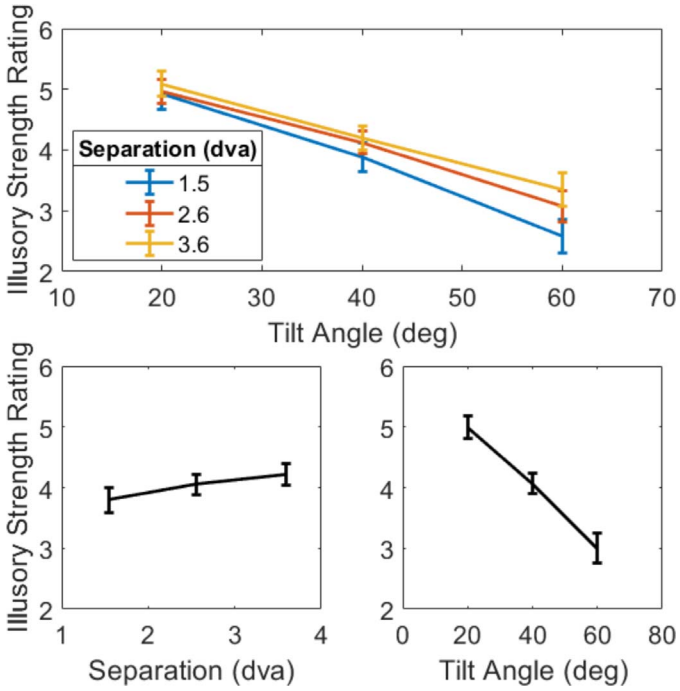

Figure 8. Top: Results from Experiment 3 for all conditions. Bottom: Data averaged across angle (left) and separation (right). Error bars are standard error of the mean.

0.055, and there was no interaction, $F(3.36, 124.16) = 1.44$, $p = 0.232$, $\eta_p^2 = 0.037$. MIC ratings decreased as a function of tilt angle.

In Experiment 2, MIC strength was found to be predicted by two factors: 3-D separation between the chevrons and their tilt. As tilt angle increased in Experiment 2, the chevron vertices moved through a smaller distance in depth. In this experiment, by changing the axis about which the objects rotated, motion through depth increased as a function of tilt angle. Nevertheless, MIC strength still decreased with increasing tilt angle. That is, weakening of MIC strength with increasing tilt angle is not due to the distance that the chevron vertex travels through depth. It may still be the case that increasing the angle of tilt reduced the perceived depth in the display, but the mechanism may not be due to the amount of motion through depth. We consider this possibility in greater detail in the general discussion.

Experiment 4

Experiments 2 and 3 suggest that that MIC clarity is strongly determined by tilt angle. At the same time, in all three experiments, there was some evidence for an additional effect of separation between vertices although the effects were in opposite directions: In Experiments 1 and 2, MIC strength decreased with increasing separation, and in Experiment 3, it increased. It is possible that the increase in Experiment 3 was due to some interaction with the different axis of rotation. It is also interesting to note that the effect of separation was much more pronounced in Experiment 2 than in either of the other experiments. Those other experiments used the same, comparatively small 3-D separations (1°–3°), and Experiment 2 tested a much larger range (4°–10°). Here, we repeat Experiment 1 except with a larger range of separations and with the difference that tilt angle, instead of being held constant, is allowed to vary. Based on the results of the previous experiments, we predicted the following interaction: If MIC strength is dominated by the recovery of 3-D structure, then when the tilt is large enough to prevent recovery of that structure, then vertex separation should have no effect on illusory strength ratings. If the tilt angle is small enough for 3-D structure to be recovered, then MIC strength will decrease with increasing separation as in Experiment 2. Note, however, that in Experiment 2, as 3-D separation increased, 2-D separation remained constant, whereas here both increase together.

Materials and methods

Participants

Participants were 19 undergraduate students at the University of California, Los Angeles (UCLA), who participated for course credit. All reported having normal or corrected-to-normal vision. All experiments were carried out in accordance with the Code of Ethics of the World Medical Association (Declaration of Helsinki) and were approved by the UCLA IRB. All participants provided informed consent.

Apparatus

Stimuli were displayed on a Viewsonic G250 CRT monitor powered by a MacPro 4 with a 2.66-GHz Quad-Core Intel Xeon processor and an NVidia GeForce GT120 graphics card. The monitor has a height of 30 cm and a width of 40 cm. The resolution of the monitor was set to 1,400 × 1,050 pixels and a refresh rate of 60 Hz. The viewing distance was 62.5 cm. These settings matched the number of pixels per degree of visual angle in the previous experiments.

Stimuli and procedure

The stimuli were chevrons as in the previous experiments. Vertical separation—3-D separation as defined in Experiment 2—and tilt angle were manipulated independently. Five vertical separations were used, 1.57°, 2.62°, 3.67°, 4.71°, and 5.76°, and five tilt

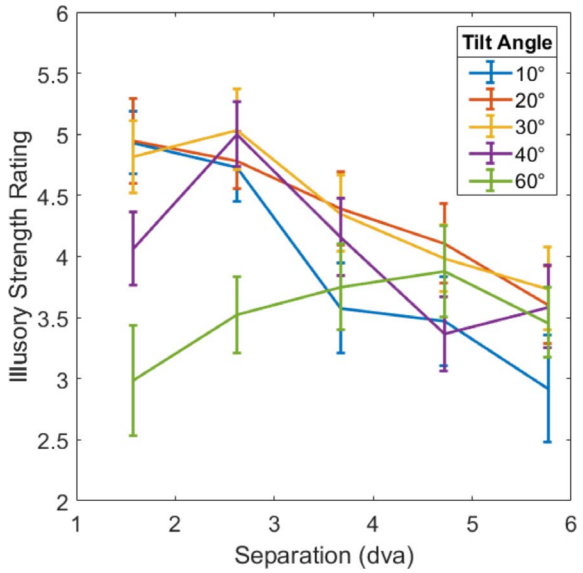

Figure 9. Results of Experiment 4. MIC illusory strength rating as a function of 3-D separation between chevron vertices. Colored lines correspond to different tilt angles. DVA = degrees of visual angle. Error bars are standard errors.

angles, 10°, 20°, 30°, 40°, and 60°. Each of the 25 unique combinations of vertical separation and tilt angle was repeated four times. The presentation order was pseudorandomized for each participant. As in Experiments 1 and 2, chevrons rotated about the axis of tilt. Inferred inducer edge length in 3-D was held constant at 1.19° for all separations and tilts. All other aspects of the displays and procedure were the same as in Experiment 1.

Results and discussion

The results of Experiment 4 are shown in Figure 9. The data were submitted to a 5 (separation) × 5 (tilt angle) repeated-measures ANOVA. There was a main effect of separation, $F(2.72, 48.98) = 8.74$, $p < 0.001$, $\eta_p^2 = 0.327$; no effect of tilt angle, $F(1.57, 28.33) = 2.43$, $p = 0.116$, $\eta_p^2 = 0.119$; and an interaction, $F(6.91, 124.31) = 4.40$, $p < 0.001$, $\eta_p^2 = 0.196$. When the chevrons were tilted by 20°, as in Experiment 1, rating strength decreased as a function of separation, replicating the results from that experiment. The effect of separation could be more clearly seen over the larger range that was tested, perhaps accounting for the comparatively smaller effects of separation on illusory strength seen in the other experiments, which only tested in the range of 1°–3°. However, the effect of separation was not uniform across tilt angles: For the largest tilt of 60°, there was no difference in ratings as a function of separation (one-way, repeated-measures ANOVA), $F(2.79, 50.29) = 1.66$, $p = 0.191$, $\eta_p^2 = 0.084$. This is in agreement with the hypothesis that, if the tilt is too large to adequately recover the 3-D arrangement of the chevrons, then image properties that might influence subsequent clarity of the MIC, such as separation, are irrelevant.

General discussion

In this study, we examined the effects of stimulus orientation, inducer edge length, vertical separation, and object tilt on the perceived strength of the MIC. MIC strength was influenced by all factors. In Experiment 1, edge length had the largest effect. Perhaps longer inducing edges led to stronger surface formation between the chevrons, which, in turn, supported the MIC. Horizontally oriented configurations were also found to produce weaker MICs than vertical or oblique ones. It was not obvious why this may have been the case and is a question for future studies. In all experiments, MIC strength decreased with increasing vertical separation between the chevrons when that distance was computed as the inferred 3-D distance between the chevron vertices. One of our empirical goals was to determine the relationship between perceived 3-D structure and the MIC. Specifically, we sought to determine whether the strength of the MIC was determined by spatial relationships defined in 2-D or 3-D coordinates. Although our derived results do not allow us to conclusively answer this question, our stimulus manipulations designed to tease these apart revealed the unexpected finding that tilt angle is a critical factor. Specifically, we found that the more tilted the object was, the weaker the contour and that this was true even if the axis of rotation was held constant (Experiment 3).

The influence of the angle of tilt was a surprising and unexpected finding. To our knowledge, this has not been an explored property of other kinds of structure-from-motion displays, which typically consist of rotating spheres or upright cylinders. A related effect might occur in stereokinetic displays in which a rotating ellipse and a dot appear to be a cone that is rotating in depth (C. L. Musatti, 1955; Zanforlin, 1988). The cone's circular base gives rise to the percept of the ellipse, and the dot is perceived as the tip of the cone. The MIC contour has previously been linked to stereokinetic displays, and both are subject to some of the same constraints, perhaps suggesting a common mechanism (Zanforlin, 2003). For example, as it relates to the MIC, illusory contours are only seen in stereokinetic displays when they undergo motion that corresponds to rotation in depth but not when they are stationary or when they translate in the frontoparallel plane (Zanforlin & Vallortigara, 1988, 1990). Likewise,

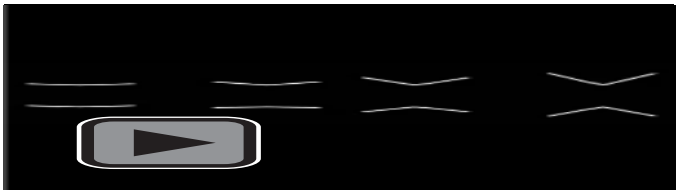

Movie 5. MIC with increasing degrees of tilt of the inducing chevrons.

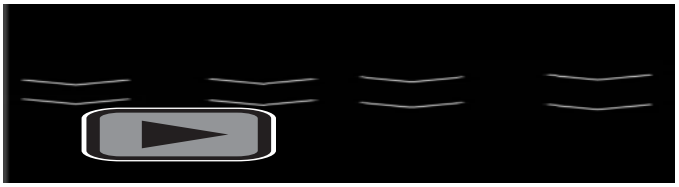

Movie 6. MIC with increasing displacement in depth between the upper and lower chevrons.

it is harder to see the rotating ellipse and dot as a cone when they are arranged as a cone viewed from the top, pointing toward the observer, i.e., with the point close to the center of the ellipse, compared to when the point is off center so that the cone is seen from the side. In the extreme case, if one were looking straight down at the cone, it would appear as a circle with a point in its center. As it rotated, there would be no change in this image and, therefore, no depth information about the height of the cone (i.e., the distance between the point and the base of the cone). If the point were slightly off center, so as to correspond to a slightly tilted cone, then the sides of the cone, like the tilted MIC, would be receding away from the observer in depth. As the point moves away from the center, the cone appears more tilted, and its sides would be more upright. The 3-D structure is easier to see in this upright just as for the upright MIC.

A similar effect occurs in stereokinetic displays with just a rotating ellipse without an accompanying point. In this case, the percept can be of a circle tilted and rotating in depth (Hildreth, 1984; C. Musatti, 1924; Wallach, Weisz, & Adams, 1956; Weiss & Adelson, 2000). Fat ellipses are more likely to be perceived as rotating in depth than narrow ellipses (Todorović, 1993; Weiss & Adelson, 2000), which is noteworthy given that fat ellipses correspond to projections of circles that are slightly tilted and narrow ellipses correspond to those that are extremely tilted. The difficulty in recovering depth from fat ellipses may be because the visual system first computes a 2-D motion flow field and only then interprets the motion in 3-D if it is consistent with the projected motion pattern of a 3-D object (Ullman, 1979). For narrow ellipses, which would correspond to a highly tilted circle, if motion flow is computed from smoothness-based algorithms, the motion pattern is not consistent with rigid 3-D rotation of that object (Weiss & Adelson, 2000). Something similar may be occurring for MIC displays with large tilts, such that the relative depth of the chevrons is difficult to recover, thereby weakening the MIC percept.

Although we did not explicitly measure the perceived depth between the chevrons, there are several reasons why this is an unlikely explanation. In Experiment 3, we tested the possibility that object tilt reduced MIC strength by reducing the amount of motion through depth of the chevrons. If the depth structure of the object—the positions in depth of the chevrons—was difficult to recover, then this could have prevented the formation of the illusory contour. In static displays that lack depth information from motion (e.g., Figure 1), no illusory contours are seen. However, even when the chevrons were set to rotate about the vertical axis so that tilting the object increased the amount of motion through depth, MIC strength was still reduced. Clear separation in depth between the two chevrons can be seen in Movie 4. Furthermore, if the chevrons are tilted independently from the illusory contour as in Figure 10A and Movie 5, there is no effect on MIC clarity. In contrast, if chevrons are placed at different depths so that their tilt is constant but the illusory contour is more tilted in depth (Figure 10B and Movie 6), then the MIC percept weakens. Taken together, these observations suggest that the relative depth of the chevrons can be recovered even at large tilts and that MIC strength depends on the orientation of the illusory contour itself, not on the orientation in depth of the visible edges.

The effect of illusory contour length on MIC strength may be related to 3-D illusory contour completion processes. It has recently been proposed that the contour interpolation mechanisms that form illusory contours take as input not 2-D contour

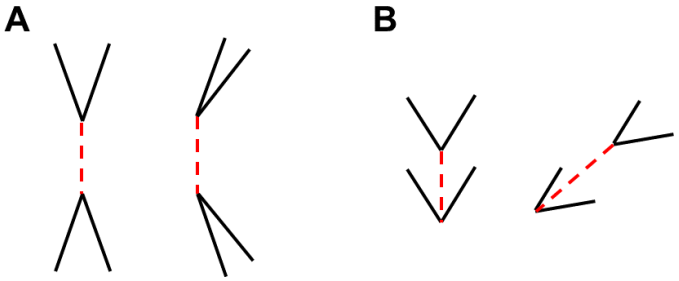

Figure 10. Examples of MIC stimuli. Black lines indicate luminance-defined edges; red, dashed lines where the illusory contour would form. (A) Front and side views of an MIC stimulus in which the inducing contours are tilted relative to the standard display. The illusory contour percept is unaffected by the tilt of the chevrons (see Movie 5). (B) Front and side views of an MIC stimulus in which one chevron is displaced in depth relative to another. The greater the separation between the chevrons, the weaker the MIC percept (see Movie 6).

position and orientation information, but, rather, their positions and orientations in depth (Kellman, Garrigan, & Shipley, 2005; Kellman, Garrigan, Shipley, et al., 2005). This suggests a multistage process for the formation of MICs. The first two stages may require analyzing 2-D motion signals and using them to recover 3-D motion, position, and orientation information. Edge terminators arranged in depth may then initiate 3-D contour interpolation and illusory contour formation. However, models for how this may occur are not readily applied to the MIC, which is unusual relative to other illusory contour displays in that the MIC appears in a different plane than the inducing edges. It is important to remember that the sequence of image transformations that produce the interpretation of the chevrons as rotating in depth does not necessitate either the formation of an illusory contour between the chevrons' vertices nor surface spreading between the inducing edges. That is, structure from motion on its own does not account for why an illusory contour is seen in these displays. Structure-from-motion models account for how depth information can be recovered from 2-D motion signals and do not make predictions about contour interpolation or the completion of illusory contours. These subsequent processes may be influenced by other properties of the object that do not directly impact the recovery of structure from motion, such as the separation between chevrons. The mechanisms by which MICs are formed remain unexplored and are a fruitful area for future research.

It is possible that there are other factors that influence MIC strength that were not considered here. For example, Klymenko and Weisstein (1984) found that the illusory contour strength depending on the angle formed by the inducers with stronger percepts associated with more acute angles. This may relate to the fact that rounding the corner also reduced the effect (Erlikhman & Caplovitz, 2018). In Experiment 1, inducer edge length was also found to influence MIC strength, and we suggested that perhaps it could be combined with separation to form a support-ratio-like measure. Given the results of subsequent experiments, it is not clear whether edge length assists in recovering the 3-D structure of the chevrons by providing more points that move through depth or whether edge length contributes to the support of illusory contour formation or both. We have recently begun to explore other features, including contrast polarity, contextual cues, surface spreading effects, and scene organization. At the moment, the extent to which MIC processing is related to other kinds of illusory contours or the stereokinetic effect remains unknown. These and earlier observations need to be taken into consideration for any computational model of form and motion, constraining models of vision.

Keywords: motion-induced contour, *stereokinetic effect*, *kinetic depth effect*, *illusory contour*, *structure from motion*

Acknowledgments

Part of this work was presented at the Vision Sciences Society 2018 conference. This research was supported by a grant to G.E. from NEI under award number F32EY025520 and EPSCoR Research Infrastructure award from the National Science Foundation to G.P.C. and M.D. under award number 1632849 and to G.P.C. under award number 1632738.

Commercial relationships: none.
Corresponding author: Gennady Erlikhman.
Email: gerlikhman@unr.edu.
Address: Department of Psychology, University of Nevada, Reno, NV, USA.

Footnote

[1] We thank an anonymous reviewer for this suggestion. Additionally, the editor suggested that a regression analysis might have more power. We did perform such an analysis for each experiment, fitting a multilevel model with participant ID as a random variable. This analysis did not change of any of the main results.

References

Anderson, B. L., & Barth, H. C. (1999). Motion-based mechanisms of illusory contour synthesis. *Neuron*, *24*(2), 433–441.

Bradley, D. R., Dumais, S. T., & Petry, H. M. (1976, May 6). Reply to Cavonoius. *Nature*, *261*(5555), 78.

Bradley, D. R., & Petry, H. M. (1977). Organizational determinants of subjective contour: The subjective Necker cube. *American Journal of Psychology*, *90*(2), 253–262.

Brainard, D. H. (1997). The psychophysics toolbox. *Spatial Vision*, *10*, 433–436.

Bruno, N., & Gerbino, W. (1991). Illusory figures based on local kinematics. *Perception*, *20*(2), 259–274, https://doi.org/10.1068/p200259.

Caganello, R., & Rogers, B. J. (1992). Anisotropies in the perception of stereoscopic surfaces: The role of

orientation disparity. *Vision Research*, *33*(16), 2189–2201.

Carman, G. J., & Welch, L. (1992, December 10). Three-dimensional illusory contours and surfaces. *Nature*, *360*(6404), 585–587.

Erlikhman, G., & Caplovitz, G. P. (2018). The motion-induced contour revisited. In J. Brown (Ed.), *Pioneer visual neuroscience: A festschrift for Naomi Weisstein* (pp. 72–87). UK: Routledge.

Erlikhman, G., Caplovitz, G. P., Gurariy, G., Medina, J., & Snow, J. C. (2018). Towards a unified perspective of object shape and motion processing in human dorsal cortex. *Consciousness & Cognition*.

Gillam, B. (1987). Perceptual grouping and subjective contours. In S. Petry & G. E. Meyer (Eds.), *The perception of illusory contours* (pp. 268–273). New York: Springer-Verlag.

Gillam, B., & Ryan, C. (1992). Perspective, orientation disparity, and anisotropy in stereoscopic slant perception. *Perception*, *21*, 427–439.

Hildreth, E. C. (1984). *The measurement of visual motion*. Cambridge, MA: MIT Press.

Hoffman, D. D., & Bennet, B. M. (1985). Inferring the relative 3-D positions of two moving points. *Journal of the Optical Society of America A*, *2*, 350–353.

Hoffman, D. D., & Bennet, B. M. (1986). The computation of structure from fixed-axis motion: Rigid structures. *Biological Cybernetics*, *54*, 71–83.

Jain, A., & Zaidi, Q. (2011). Discerning nonrigid 3D shapes from motion cues. *Proceedings of the National Academy of Sciences, USA*, *108*(4), 1663–1668.

Kanizsa, G. (1955). Margini quasi-percettivi in campi con stimolazione omogenea. *Rvista di Psicologia*, *49*, 7–30.

Kanizsa, G. (1979). *Organization in vision*. New York: Praeger.

Kellman, P. J., Garrigan, P., & Shipley, T. F. (2005). Object interpolation in three dimensions. *Psychological Review*, *112*(3), 586–609.

Kellman, P. J., Garrigan, P., Shipley, T. F., Yin, C., & Machado, L. (2005). 3-D interpolation in object perception: Evidence from an objective performance paradigm. *Journal of Experimental Psychology: Human Perception and Performance*, *31*, 558–583.

Kellman, P. J. & Shipley, T. F. (1991). A theory of visual interpolation in object perception. *Cognitive Psychology*, *23*, 141–221.

Klymenko, V., & Weisstein, N. (1980). Illusory contour produced by rotation-in-depth [Abstract]. *Optics News*, *6*(3), 61.

Klymenko, V., & Weisstein, N. (1981). The motion-induced contour. *Perception*, *10*, 627–636.

Klymenko, V., & Weisstein, N. (1983). The edge of an event: Invariants of a moving illusory contour. *Perception & Psychophysics*, *34*(2), 140–148.

Klymenko, V., & Weisstein, N. (1984). The razor's edge: A dichotomy between monohedral and dihedral edge perception. *Vision Research*, *24*(9), 995–1002.

Klymenko, V., Weisstein, N., & Ralston, J. V. (1987). Illusory contours, projective transformations, and kinetic shape perception. *Acta Psychologica*, *64*, 229–243.

McCarthy, J. D., Erlikhman, G., & Caplovitz, G. P. (2017). The maintenance and updating of representations of no longer visible objects and their parts. In C. J. Howard (Ed.), *Progress in brain research, vol. 236* (pp. 163–192). Elsevier.

McCarthy, J. D., Strother, L., & Caplovitz, G. P. (2015). Spatiotemporal form integration: Sequentially presented inducers can lead to representations of stationary and rigidly rotating objects. *Attention, Perception, & Psychophysics*, *77*(8), 2740–2754.

Mitchison, G. J., & McKee, S. P. (1990). Mechanisms underlying the anisotropy of stereoscopic tilt perception. *Vision Research*, *30*, 1781–1791.

Musatti, C. (1924). Sui fenomeni stereocinetici. *Archivio Italiano di Psicologia*, *3*, 105–120.

Musatti, C. L. (1955). La stereocinesi e il problema della struttura dello spazio visibile. *Rivista dipsicologia*, *49*, 3–57.

Pelli, D. G. (1997). The video toolbox software for visual psychophysics: Transforming numbers into movies. *Spatial Vision*, *10*, 437–442.

Poom, L. (2001a). Visual inter-attribute contour completion. *Perception*, *30*(7), 855–865.

Poom, L. (2001b). Visual summation of luminance lines and illusory contours induced by pictorial, motion, and disparity cues. *Vision Research*, *41*(28), 3805–3816.

Ramachandran, V. S. (1986). Capture of stereopsis and apparent motion by illusory contours. *Perception & Psychophysics*, *39*(5), 361–373.

Rogers, B., & Graham, M. E. (1983, September 30). Anisotropies in the perception of three-dimensional surfaces. *Science*, *221*(4618), 1409–1411.

Rokers, B., Yuille, A., & Liu, Z. (2006). The perceived motion of a stereokinetic stimulus. *Vision Research*, *46*, 2375–2387.

Rubin, N. (2001). The role of junctions in surface completion and contour matching. *Perception*, *30*, 339–366.

Shipley, T. F. & Kellman, P. J. (1990). The role of discontinuities in the perception of subjective figures. *Perception & Psychophysics*, *48*, 259–270.

Shipley, T. F., & Kellman, P. J. (1992). Strength of visual interpolation depends on the ratio of physically specified to total edge length. *Perception & Psychophysics*, *52*, 97–106.

Todorović, D. (1993). Analysis of two- and three-dimensional rigid and nonrigid motions in the stereokinetic effect. *Journal of the Optical Society of America A*, *10*, 804–826.

Tse, P. (1998). Illusory volumes from conformation. *Perception*, *27*, 977–992.

Tse, P. (1999). Volume completion. *Cognitive Psychology*, *39*, 37–68.

Tse, P. (2017a). Dynamic volume completion and deformation. *i-Perception*. Retrieved from https://doi.org/10.1177/2041669517740368.

Tse, P. (2017b). Volume completion between contour fragments at discrete depths. *i-Perception*. Retrieved from https://doi.org/10.1177/2041669517747001.

Ullman, S. (1979). *The interpretation of visual motion*. Cambridge, MA: MIT Press.

Ullman, S. (1984a). Maximizing rigidity: The incremental recovery of 3-D structure from rigid and non-rigid motion. *Perception*, *13*, 255–274.

Ullman, S. (1984b). Rigidity and misperceived motion. *Perception*, *13*, 219–220.

Vogels, R., & Orban, G. A. (1987). Illusory contour orientation discrimination. *Vision Research*, *27*(3), 453–467.

Wallach, H., & Bacon, J. (1973). Two forms of retinal disparity. *Perception & Psychophysics*, *19*, 375–382.

Wallach, H., & O'Connell, D. N. (1953). The kinetic depth effect. *Journal of Experimental Psychology*, *45*(4), 205–217.

Wallach, H., Weisz, A., & Adams, P. A. (1956). Circles and derived figures in rotation. *American Journal of Psychology*, *69*, 48–59.

Yin, C., Kellman, P. J., & Shipley, T. F. (2000). Surface integration influences depth discrimination. *Vision Research*, *40*(15), 1969–1978.

Zanforlin, M. (1988). The height of a stereokinetic cone: A quantitative determination of a 3-D effect from 3-D moving patterns without a "rigidity assumption." *Psychological Research*, *50*, 162–172.

Zanforlin, M. (2003). Stereokinetic anomalous contours: Demonstrations. *Axiomathes*, *13*, 389–398.

Zanforlin, M., & Vallortigara, G. (1988). Depth effect from a rotating line of constant length. *Perception & Psychophysics*, *44*(5), 493–499.

Zanforlin, M., & Vallortigara, G. (1990). The magic wand: A new stereokinetic anomalous surface. *Perception*, *19*, 447–457.